Sensor and Simulation Notes

Note 479

October 2003

A Dual-Polarity Impulse Radiating Antenna

Leland H. Bowen and Everett G. Farr
Farr Research, Inc.

Dean I. Lawry
Air Force Research Laboratory, Directed Energy Directorate

Abstract

We describe here the construction and testing of an IRA with dual polarity. Four feed arms are evenly spaced around the reflector, and each channel consists of a pair of arms on opposite sides of the reflector. Each channel uses a standard balun to convert the 50-ohm input impedance to 200 ohms. Since the characteristic impedance of each channel is 400 ohms, there is a 2:1 impedance mismatch at the feed point. Our measurements demonstrate that, despite the impedance mismatch, the dual-polarity IRA is a viable antenna. We present here the experimental results of the dual polarity IRA, and we compare them to those of a standard IRA-1, upon which the dual-polarity IRA is based.

I. Introduction

Dual polarity Impulse Radiating Antennas may be useful in a variety of applications, such as UWB radar, and target identification. Adding a second polarization to a single antenna essentially provides twice the information with the same aperture area. Until now, no design has been built and tested, so we report here the results of the first dual-polarity IRA.

Until now, we have not tried to construct an IRA with dual polarity, due to the difficulty of maintaining a good impedance match throughout the antenna. However, we recently built a poorly matched IRA with a single unbalanced 50-ohm feed, with surprisingly good results [1]. These results inspired us to try a dual-polarity IRA, in hopes that any mismatch at the feed point might be tolerable for those applications where reflections within the system are not of great importance.

The dual-polarity IRA described here, designated IRA-1D, is very similar to the IRA-1 developed by Farr Research, Inc. [2, 3]. For the IRA-1D we used the same feed arm configuration as used on the IRA-1, which had four feed arms spaced uniformly around the aperture, with the electrical center of the feed arms intersecting the edge of the reflector. The only difference in the IRA-1D is that each pair of opposite feed arms is connected to a separate 50-to-200-ohm balun. This produces a mismatch from 200 to 400 ohms at the focus of the reflector on each channel. In spite of this 2:1 impedance mismatch, the antenna characteristics of the IRA-1D are quite good up to at least 10 GHz. We provide here the antenna characteristics for both polarizations of the IRA-1D, and we compare these results to those of the standard IRA-1. We also compare the IRA-1D to other versions of the 18-inch IRA reported in [3].

The IRA-1D is an experimental antenna used to determine the viability of the dual polarity configuration for use on a larger (1.21 m) diameter collapsible antenna intended to be deployed in space. The larger antenna will be an Ultra-Compact IRA (UCIRA) which will collapse into a very compact package for stowage during launch, and will then deploy on command. Since the UCIRA requirements are well below 10 GHz, we plan to use a configuration similar to the IRA-1D in the design of the UCIRA. Although the dual polarity experiments were conducted with a particular antenna in mind, the data presented here may be of interest in numerous other applications.

We begin now describing the IRA-1D.

II. Description

We begin by describing the physical characteristics of the IRA-1D. This antenna uses the same 0.46 m (18 in.) diameter spun aluminum reflector as the IRA-1. For this reflector, F/D = 0.5 which gives a focus of 0.23 m (9 in.) and depth of 57.5 mm (2.26 in.). As with the IRA-1, the feed arms are spaced 90° apart. However, for the dual polarity version, the antenna has been rotated 45° so that one pair of feed arms is in the vertical plane and the other pair is in the horizontal plane. Two separate splitter baluns are used for the dual polarity feed. One splitter feeds the vertical pair of feed arms, while the other splitter feeds the horizontal pair. Each splitter divides the signal from a 50-ohm connector onto two 100-ohm semi-rigid coax cables in parallel. The other ends of these cables are connected in series to provide a 200-ohm impedance at the feed point. This provides a 2:1 impedance mismatch between the 200-ohm balun output and the 400-ohm impedance of a single feed arm pair.

The feed arm pairs can be treated independently, since each pair of feed arms are perpendicular to the other pair. In other words, each pair of feed arms lies on a plane of symmetry with respect to the other pair. Thus, to analyze one pair, the other pair is ignored. This configuration is identical to the coplanar conical plates shown in Figure 9 of [4]. The feed arms for the IRA-1D are the same as those used for the standard IRA-1 with $\beta_0 = 53.13°$, $\beta_1 = 46.86°$, and $\beta_2 = 59.95°$. The included angle of the feed arms for this configuration is $\beta_2 - \beta_1 = 13.1°$. This is similar to the example on page 22 of [4] except that in our case F/D = 0.5 rather than 0.4 as used in the example. In either case, the characteristic impedance of the feed arm pair is 400 Ω.

We considered using a 200-ohm impedance on a single pair of feed arms, in order to match to the 200-ohm output of the balun. However, this would have required extremely wide feed arms, resulting in higher aperture blockage and increased difficulty in construction. Therefore, we decided to use the standard feed arms and accept the compromise of the impedance mismatch. Each feed arm is terminated with a 200-ohm distributed load resistance.

In Figure 1 we show the front and back sides of the IRA-1D. In the picture on the left, one can see two of the semi-rigid coax feed cables attached to the feed arms. The other two feed cables are inside the center support tube. The feed cables are connected to the feed arm tips at the apex or focus of the reflector. A second cable for each feed arm pair is fed up the center support, so it is not visible. In the picture on the right one can see the two splitters. The one near the top feeds the vertical channel, while the one to the right feeds the horizontal channel. Detail of the feed point is shown in Figure 2. The center conductor wires from the 100-ohm semi-rigid coax are so small that the connections to the tips of the feed arms cannot be seen clearly, even in this enlarged picture. However, the figure does illustrate the vertical and horizontal polarities of the antenna.

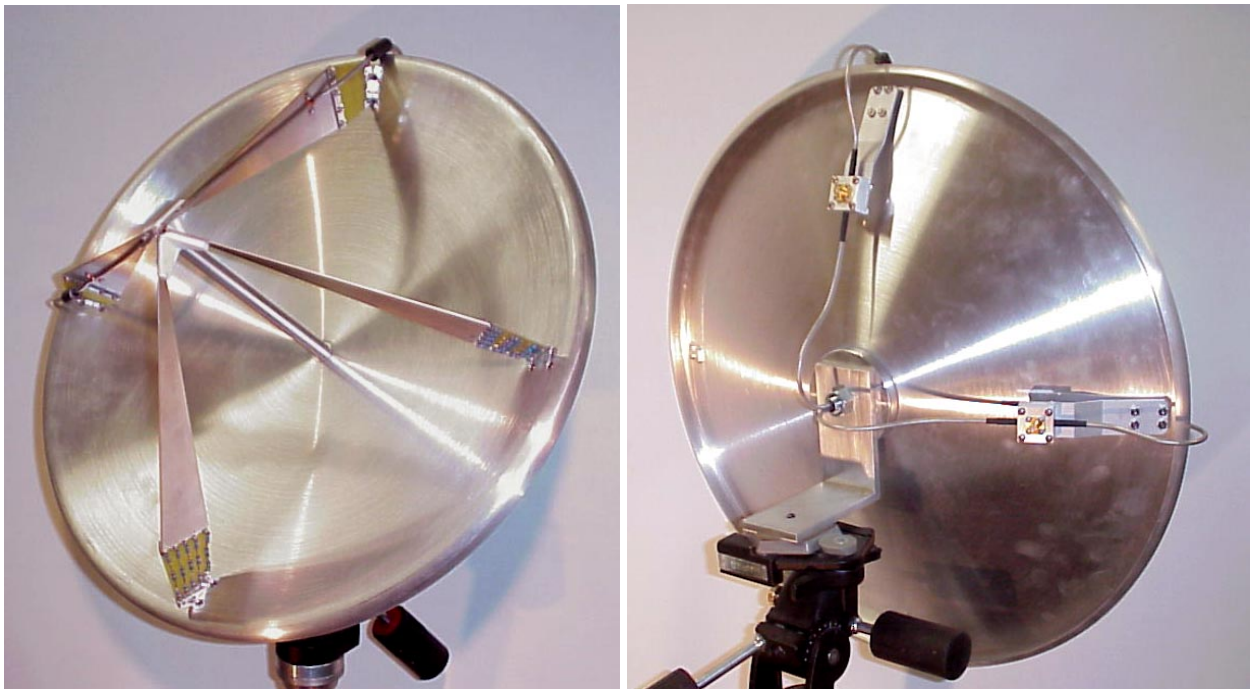

Figure 1. IRA-1D, front and back showing dual polarization feeds.

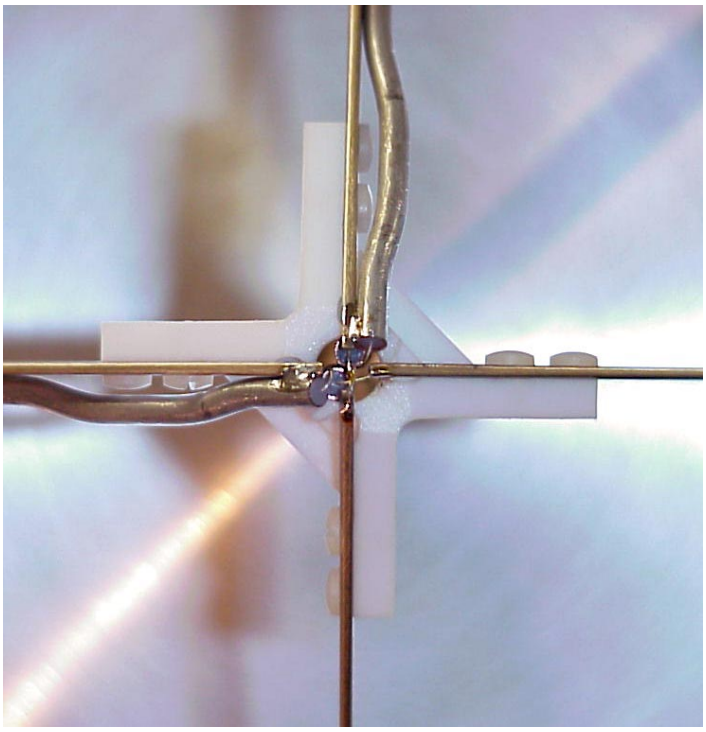

Figure 2. Detail of IRD-1D feed point.

III. IRA-1D Antenna Characteristics

The antenna characteristics were measured on the Farr Research outdoor time domain antenna range. The source was a Farr Research TEM-1-50 sensor driven by a Picosecond Pulse Labs Model 4015C high-speed pulse generator. The 4015C has a negative 4 V output with a fall time of around 20 ps. The IRA-1D was used as the receiver. The antennas were 10 meters apart and 3 meters above the ground. The data were recorded using a Tektronix TDS8000 digital sampling oscilloscope with an 80E04 sampling head. First, we measured the characteristics of the vertical channel (V), and then we measured the characteristics of the horizontal channel (H).

We began our measurements by measuring the TDR of the antenna. In Figure 3 we show the TDR of the vertical channel of the antenna. The mismatch at the splitter is minimal, but the mismatch at the feed point is more substantial, and we can identify two reasons for this. First there is a spike in the impedance right at the feed point due to the complexity of the feed point connections and the proximity of the connections for the other polarity. Second there is a large jump in impedance due to the mismatch between the 200-ohm impedance at the balun output and the 400-ohm impedance of the pair of feed arms. There is also a dip in the impedance at the end of the feed arms, where the 200-ohm load resistors are attached. This dip is followed by a relatively flat impedance. This part of the TDR occurs after the pulse has reached the reflector.

The normalized impulse response of the vertical channel is shown in Figure 4. The peak for the vertical section of the antenna is somewhat better than that of the standard IRA-1 and the FWHM is about the same. The comparable data for the IRA-1 is provided later in this paper in Figures 17 through 19.

The effective and standard gains of the vertical channel of the IRA-1D are shown in Figures 5 and 6. In each case, the gains are displayed using both linear and logarithmic frequency scales. The gain and effective gain are almost identical, with only slight variations at high frequencies. The gain plots for the IRA-1D are slightly better than those of the standard IRA-1 (see Figures 19 and 20 later in this paper). The average cross-polarization rejection is almost exactly the same, although it is not as good at the high end. The crosspol gain is somewhat noisier for the IRA-1D. For completeness we show the S_{11} and antenna factor for the IRA-1D in Figures 7 and 8.

In Figure 9 we show the normalized pattern plots for the H and E planes. The beam width is somewhat greater in the H plane than in the E plane. Some side lobes are evident in the E plane pattern.

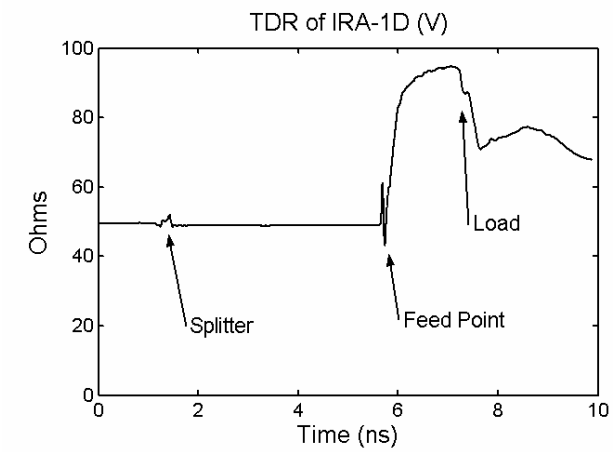

Figure 3. TDR of the IRA-1D (Vertical).

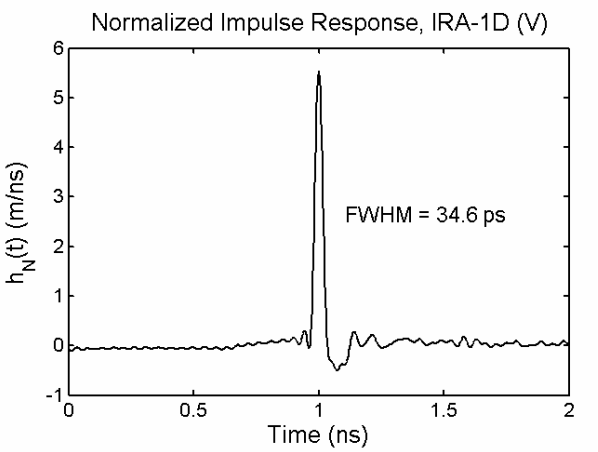

Figure 4. Normalized Impulse Response (V).

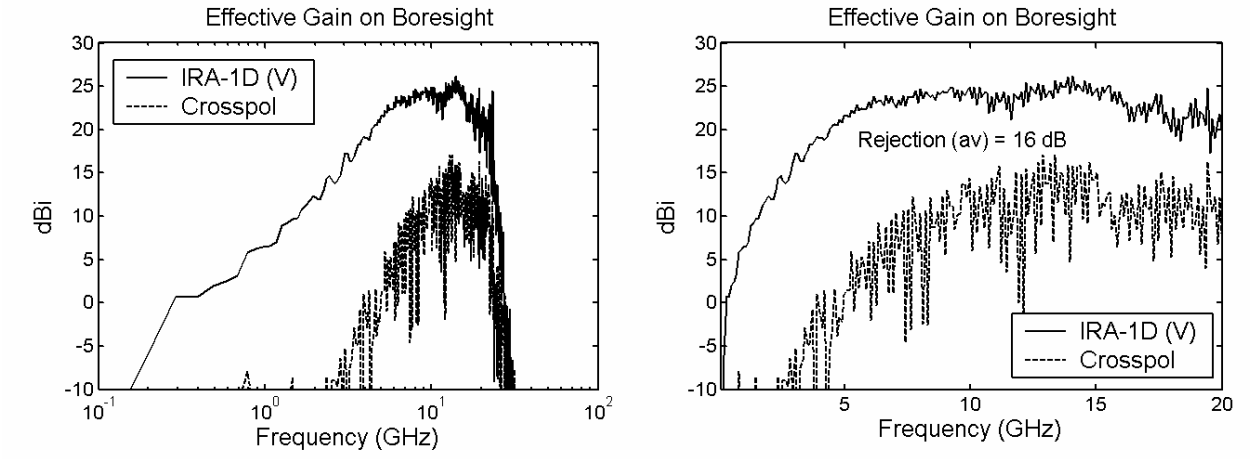

Figure 5. Effective Gain on boresight for the IRA-1D (Vertical).

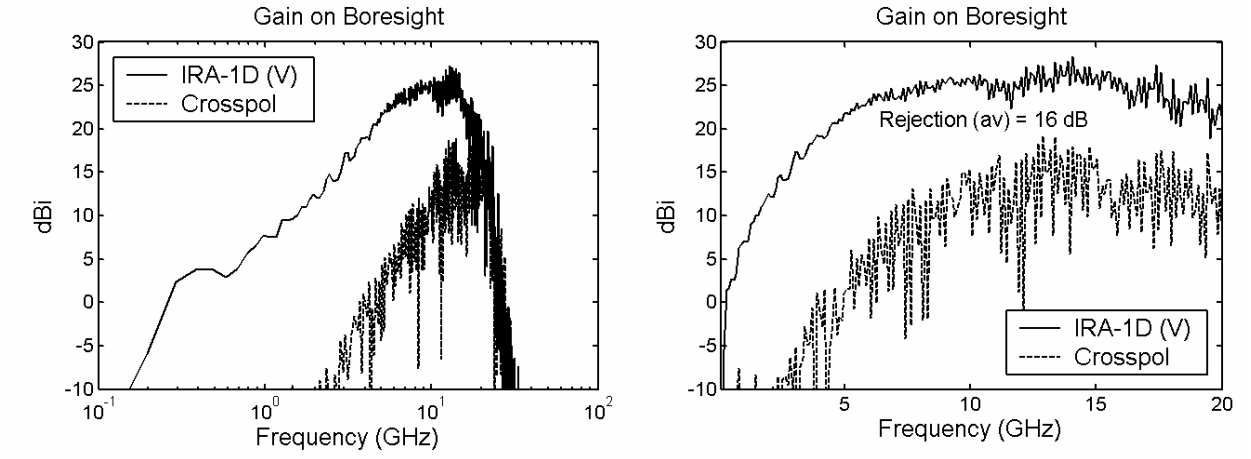

Figure 6. Gain on boresight for the IRA-1D (Vertical).

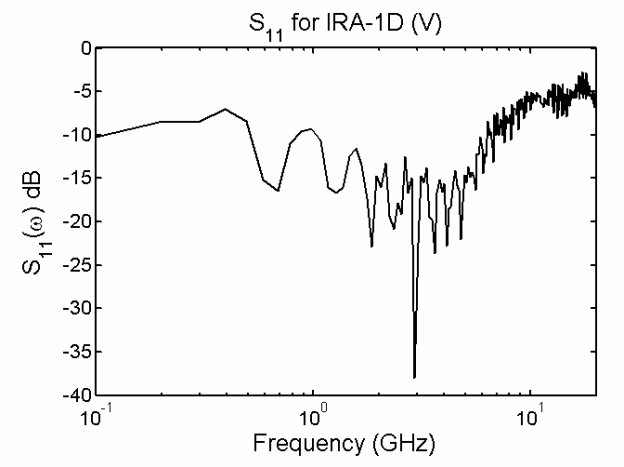

Figure 7. S_{11} for the IRA-1D (Vertical).

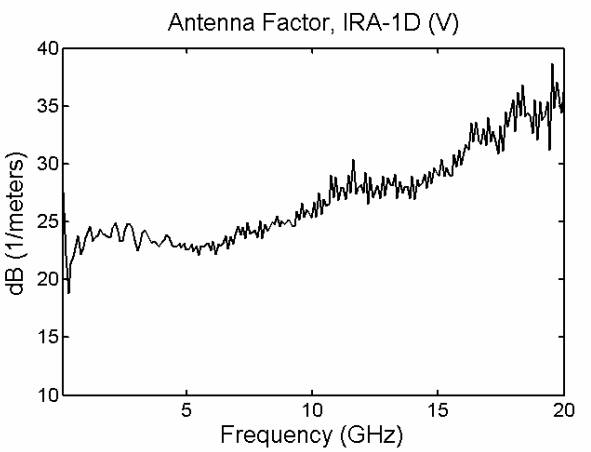

Figure 8. Antenna Factor for the IRA-1D (V).

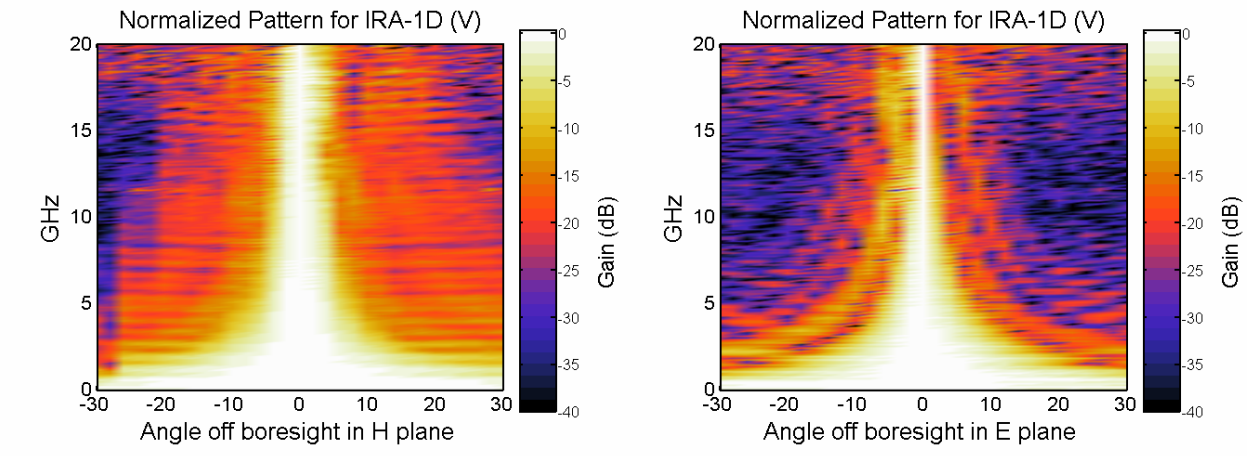

Figure 9. Normalized pattern in the H and E planes for the IRA-1D (Vertical).

Now we consider data on the horizontal channel. The TDR, shown in Figure 10, is much the same as that shown in Figure 3 for the vertical polarity. However, the normalized impulse response, shown in Figure 11, has a lower peak and a considerably greater FWHM. Ideally, we would like the two channels to have the same characteristics. However, one feed must be behind the other, so one feed must be slightly out of focus.

In Figures 12 and 13 we show the effective and standard gains for the horizontal polarity. As with the vertical polarity there is almost no difference between the effective gain and the standard gain. The peak gain for the horizontal channel of the antenna is somewhat lower than that of the vertical section, and it drops rather drastically above about 12 GHz. However, below 6 GHz both the copol gains and the crosspol gains are almost identical for the two polarities. The crosspol gain is higher than the copol gain above about 12 GHz for the horizontal polarization. This is a rather strange behavior and is probably related to the wiring and support configuration at the feed point (Figure 2).

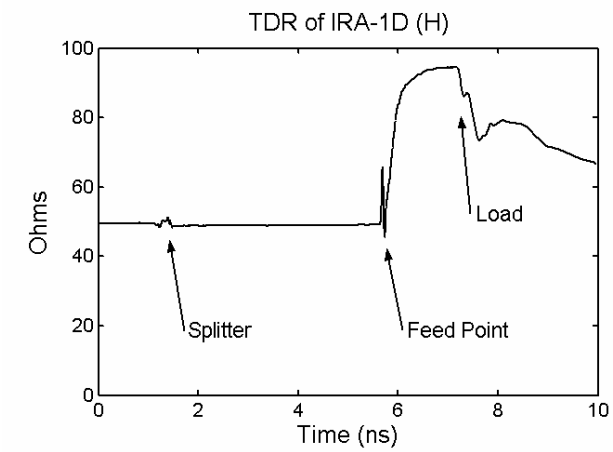

Figure 10. TDR of the IRA-1D (Horizontal).

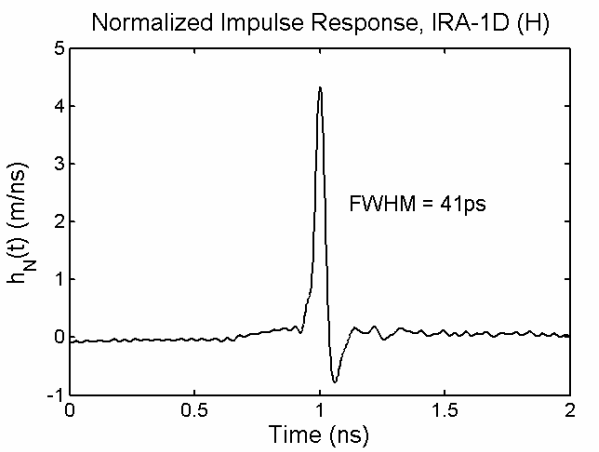

Figure 11. Normalized Impulse Response.

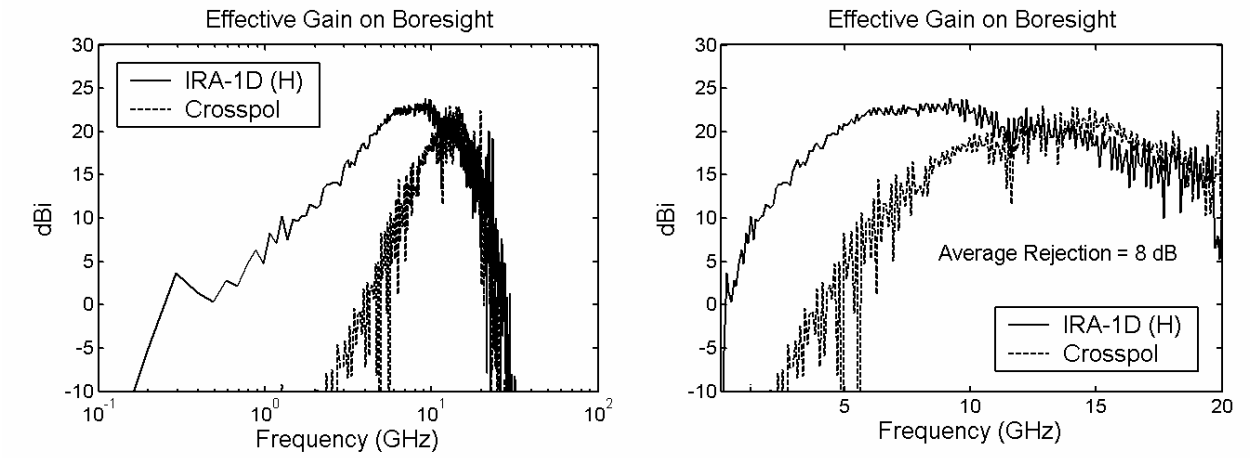

Figure 12. Effective Gain on boresight for the IRA-1D (Horizontal).

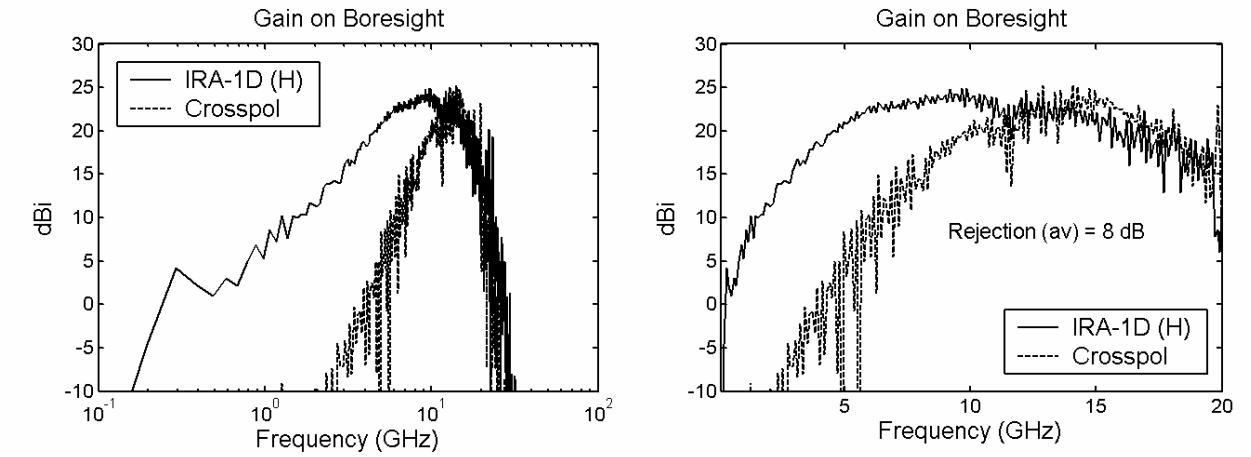

Figure 13. Gain on boresight for the IRA-1D (Horizontal).

We show the S_{11} and antenna factor for the horizontal section of the IRA-1D in Figures 14 and 15. The S_{11} characteristics are similar for the two polarities. The antenna factors are about the same for low frequencies but at the high end the antenna factor for the horizontal polarization is about 10 dB higher. The pattern plots in Figure 16 show that, as with the vertical polarity, the beamwidth is narrower in the E plane than the H plane and there are some side lobes in the E plane. Also, we see that above about 14 GHz the pattern becomes quite noisy. This is probably related to the strange behavior of the gains above 12 GHz as noted in the last paragraph. There are several measurements in the E plane for which the data are lower than expected. This causes the dark areas on the left side of the E plane plot.

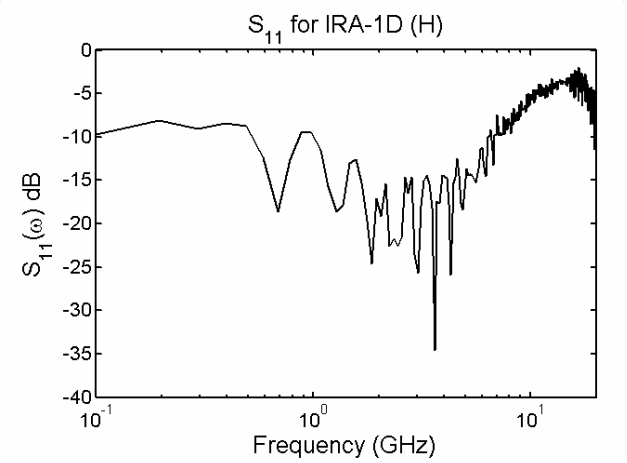

Figure 14. S_{11} for the IRA-1D (Horizontal).

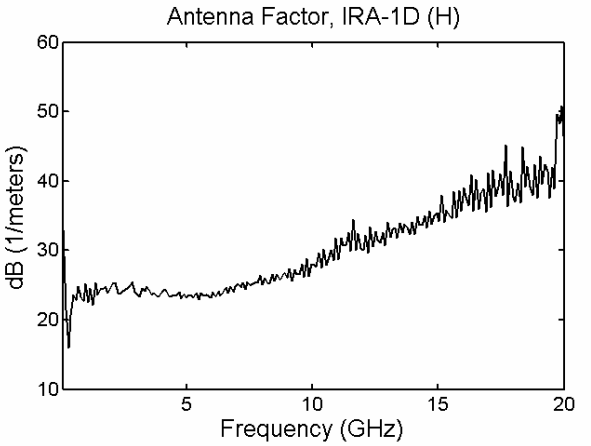

Figure 15. Antenna Factor for the IRA-1D.

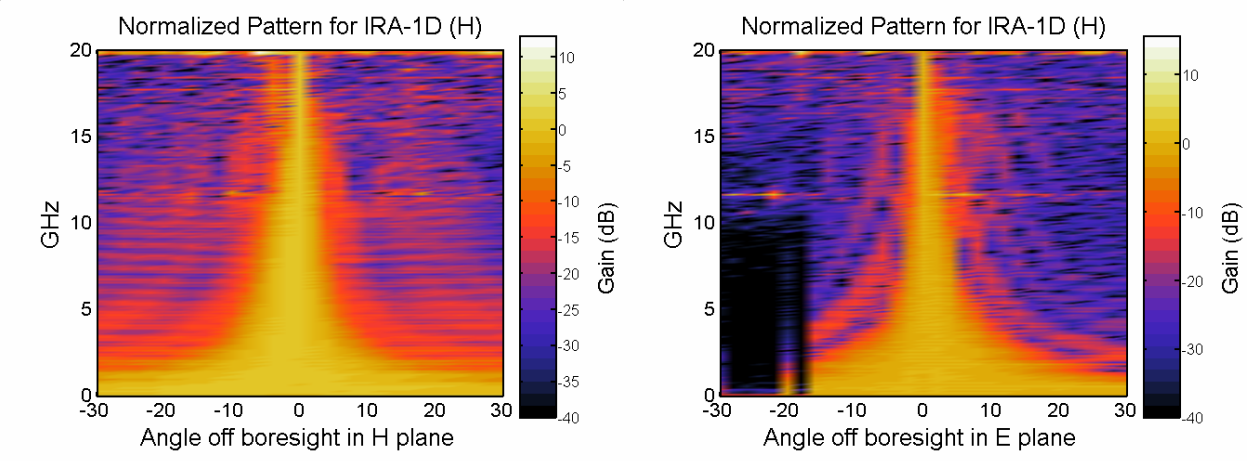

Figure 16. Normalized pattern in the H and E planes for the IRA-1D (Horizontal).

Next, we show some of the characteristics of the standard IRA-1, on which the IRA-1D is based. In Figure 17 we plot the TDR of the IRA-1 using the same scale as that used for Figures 3 and 10 for ease of comparison. The overall TDR is much flatter, since the 200-ohm characteristic impedance of the antenna is matched to the 200-ohm feed impedance of the balun. The impedance match at the splitter is not as good as with the IRA-1D since an older version of the splitter was used on the IRA-1.

The peak of the normalized impulse response shown in Figure 18 lies between the values for the vertical and horizontal polarizations of the IRA-1D, shown in Figures 4 and 11, respectively. The FWHM is almost exactly the same as that for the vertical polarization of the IRA-1D. One would expect the IRA-1 to be better in all cases, due to the better impedance match. However, the IRA-1 used for these measurements was an experimental version with an added dummy cable to improve the symmetry [3]. Perhaps the older splitter and possible variations in the construction at the feed point can account for the overall slightly lower performance of the IRA-1.

The gain characteristics of the IRA-1 in Figure 19 are similar to those of the IRA-1D, as shown in Figures 6 and 13 up to about 10 GHz. For easier comparison, we overlaid these gains in Figure 20. The gains for both polarities of the IRA-1D and the IRA-1 are almost identical up to 6 GHz. The impedance mismatch at the feed point of the IRA-1D has little impact to its overall characteristics, except at frequencies above about 10 GHz.

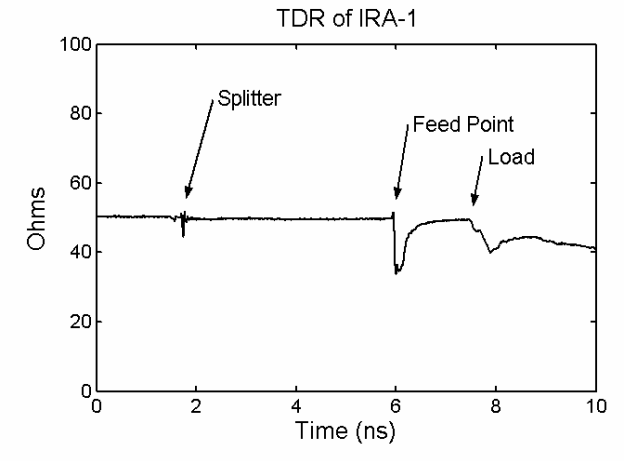

Figure 17. TDR of the IRA-1.

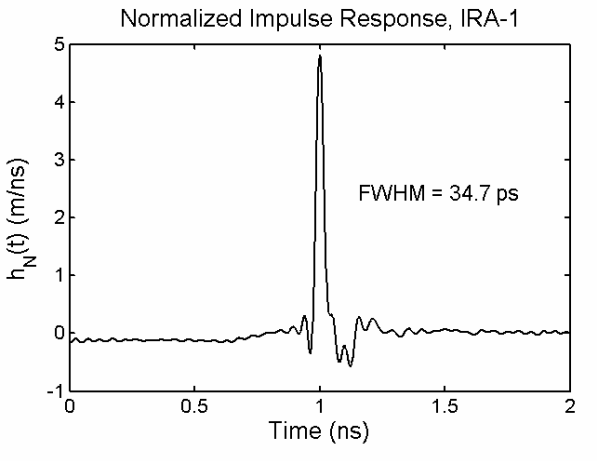

Figure 18. Normalized Impulse Response of the IRA-1

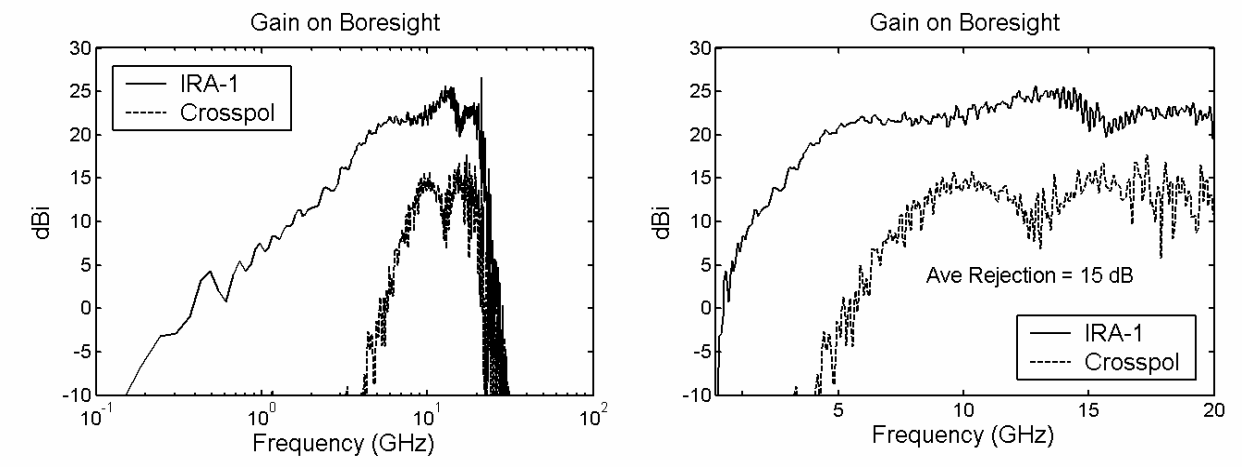

Figure 19. Gain on boresight for the IRA-1.

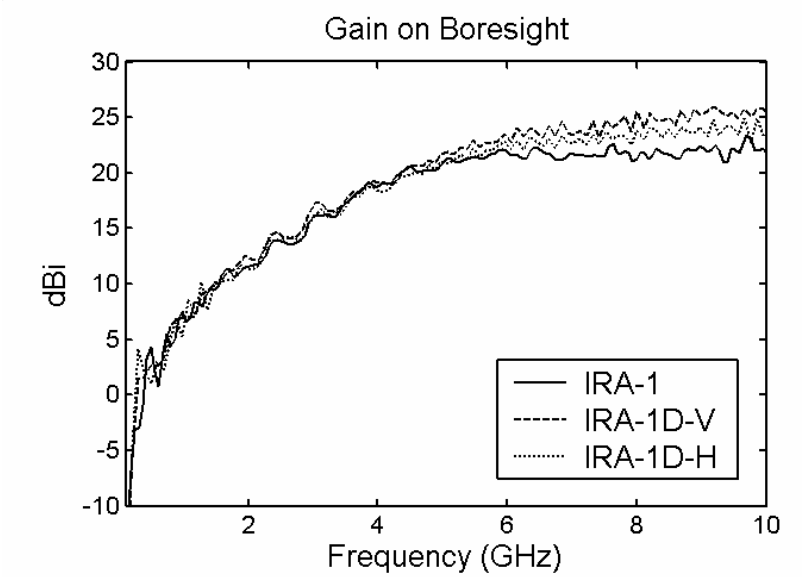

Figure 20. Gain on boresight for the IRA-1, IRA-1D (V), and IRA-1D (H).

IV. Discussion.

The variation between the vertical and horizontal polarizations is greater than we would like, especially above 10 GHz. However, we have shown that the dual-polarity configuration is viable for certain applications. The variation between the two antenna channels may be reduced by improving the construction of the feed point.

The construction of the feed point is critical for good high frequency response. There are two features in the design that limit the antenna performance, both of which deal with the coax cables between the splitter and the feed point. First, the lengths of the cables must be the same, so the pulses from each cable arrive at the feed point at exactly the same time. Second, the lengths of the exposed center conductors at the feed point must be kept as short as possible, and must also be the same length.

The dual polarity configuration requires that the two feeds cross each other at the feed point. This means that one of the center conductors must pass in front of the other. In this case, the vertical feed is positioned in front of the horizontal feed. To make the wire on the vertical polarization reach, the center conductor had to be 2-3 mm longer than the other wire. This should have created some problems at high frequencies; however, the vertical channel had the best performance, especially at high frequencies.

It may be possible to rebuild the feed point so the lengths of the exposed wires are more even. If we accomplish this, then the characteristics of the V and H channels of the antenna should match more closely, and the crosspol on each channel should decrease. This modification is challenging to implement, due to the very small space available to make connections at the feed point. Note also that the symmetry of the feed arms, feed cables, and the plastic feed-point supports could be improved. This may improve the crosspol rejection [5].

V. Conclusions

Our experiments with the IRA-1D show that the dual polarization configuration for the IRA is a viable alternative for applications where an impedance mismatch can be tolerated. The copol gain for both polarities of the IRA-1D and the IRA-1 are almost identical up to 5 GHz. The response of the two channels is not identical, but it is close enough for many applications.

The dual-polarity configuration will be developed more fully for use on the UCIRA (Ultra-Compact IRA). The configuration of the feed will be somewhat different for the UCIRA, since we plan to use a twinline feed for that antenna. The twinline feed has the advantage of being more flexible than coax cables, and it can be constructed to have the desired 200-ohm impedance [6]. The feed point design can be improved on this version, because there will be fewer cables converging at the focus. This will reduce the differences between the two channels, however, this may not be critical for our intended application on the UCIRA. The frequency range for this antenna does not extend above 10 GHz, and the two polarities are already quite similar below this frequency.

Acknowledgements

We wish to thank the Air Force Research Laboratory, Directed Energy Directorate, for funding this work.

References.

1. L. H. Bowen, L. M. Atchley, E. G. Farr, D. E. Ellibee, W. J. Carey, J. R. Mayes and L. L. Altgilbers, “A Prototype High-Voltage UWB Transmitter”, Sensor and Simulation Note 473, March 2003.

2. L. H. Bowen, E. G. Farr, C. E. Baum, T. C. Tran, and W. D. Prather “Experimental Results of Optimizing the Location of Feed Arms in a Collapsible IRA and a Solid IRA”, Sensor and Simulation Note 450, November 2000.

3. L. H. Bowen, E. G. Farr, C. E. Baum, T. C. Tran, and W. D. Prather, “Results of Optimization Experiments on a Solid Reflector IRA”, Sensor and Simulation Note 463, January 2002.

4. E. G. Farr, and C. E. Baum, “Prepulse Associated with the TEM Feed of an Impulse Radiating Antenna”, Sensor and Simulation Note 337, March 1992.

5. C. E. Baum, Symmetry in Single-Polarization Reflector Impulse Radiating Antennas, Sensor and Simulation Note 448, July 2000.

6. L. H. Bowen, E. G. Farr, J. P. Paxton, A. J. Witzig, C. E. Baum, D. I. Lawry, and W. D. Prather, “Fabrication and Testing of a Membrane IRA”, Sensor and Simulation Note 464, January 2002.